Electronic Supplementary Material (ESI) for Materials Horizons.

Supplementary Information:

The role of traps in the photocurrent generation mechanism in thin InSe photodetectors

Qinghua Zhao, Wei Wang, Felix Carrascoso-Plana, Wanqi Jie, Tao Wang, Andres Castellanos-Gomez*, Riccardo Frisenda**

Q. Zhao, Wei Wang, Prof. W. Jie, Prof. T. Wang
State Key Laboratory of Solidification Processing, Northwestern Polytechnical University, Xi'an, 710072, P. R. China
Key Laboratory of Radiation Detection Materials and Devices, Ministry of Industry and Information Technology, Xi'an, 710072, P. R. China
E-mail: taowang@nwpu.edu.cn

Q. Zhao, F. Carrascoso-Plana, Dr. R. Frisenda, Dr. A. Castellanos-Gomez
Materials Science Factory. Instituto de Ciencia de Materiales de Madrid (ICMM-CSIC), Madrid, E-28049, Spain.

E-mail: andres.castellanos@csic.es; riccardo.frisenda@csic.es

Table of contents

Section S1 – InSe photodetectors from the literature

Table S1: The photoresponsivity and response time of various thin InSe photodetectors with metal-InSe-metal geometry found in literature.

Reference	Device geometry	Wavelength	Response time	Responsivity
30	Al-InSe-Al	543 nm	87 µs	---
31	Metal-InSe-metal	532 nm	488 µs	34.7 mA W^{-1}
32	Cr/Au-InSe-Cr/Au	450 nm	50 ms	6.9 – 157 A W^{-1}
33	Cr/Au-InSe-Cr/Au	515.6 nm	---	~ 10^7 A W^{-1}
35	Cr/Au-InSe-Cr/Au	700 nm	5 ms	~ 10^4 A W^{-1}
36	Au-InSe-Au	370 nm	0.5 s	27 A W^{-1}
37	Ti/Au-InSe-Ti/Au	500 nm	5.63 s	700 A W^{-1}
42	Pt/Au/Pt	325 nm	---	~ 10^7 A W^{-1}
37	G-InSe-G	500 nm	120 µs	60 A W^{-1}
38	G-InSe-G	633 nm	1 ms	4000 A W^{-1}

Section S2 – Structural characterization of InSe photodetectors

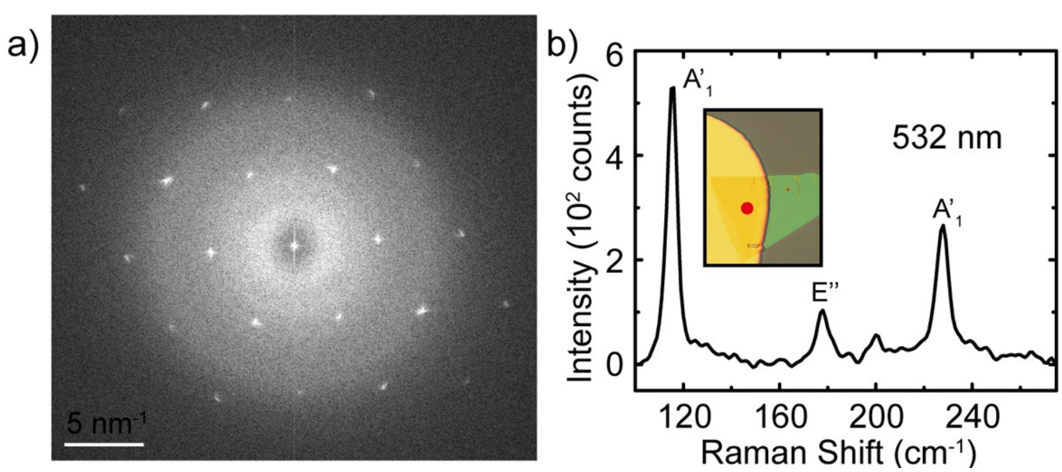

Figure S1: Crystal structure characterizations of thin InSe flakes. (a) The diffraction pattern of thin InSe flake by transmission electron microscope (TEM). The hexagonal geometry of the pattern indicates that the InSe is β or ε phase. (b) The Raman spectra of thin InSe flake on Au. The peak centered at 200 cm^{-1} gives the confirmation that the InSe is ε phase.

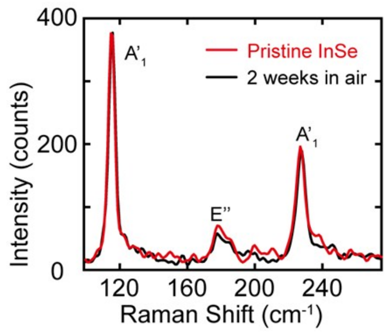

Figure S2: Raman spectra (532 nm laser, power density 0.11 mW μm^{-2}) of the InSe flake shown in Figure 1(b) on SiO_2/Si substrate recorded in the pristine state and after two weeks in air conditions.

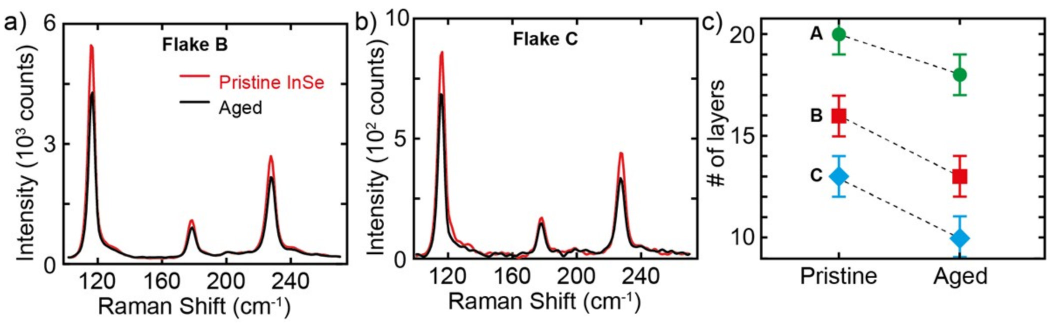

Figure S3: (a-b) Raman spectra (532 nm laser, power density 0.11 mW μm^{-2}) of two InSe flakes in pristine conditions and after 10 days in air. (c) Estimation of the thickness (number of layer) of pristine and aged InSe flakes. In average we observe a loss of 2-3 layers after aging the sample in air.

Section S3 – Optoelectronic characterization of InSe photodetectors

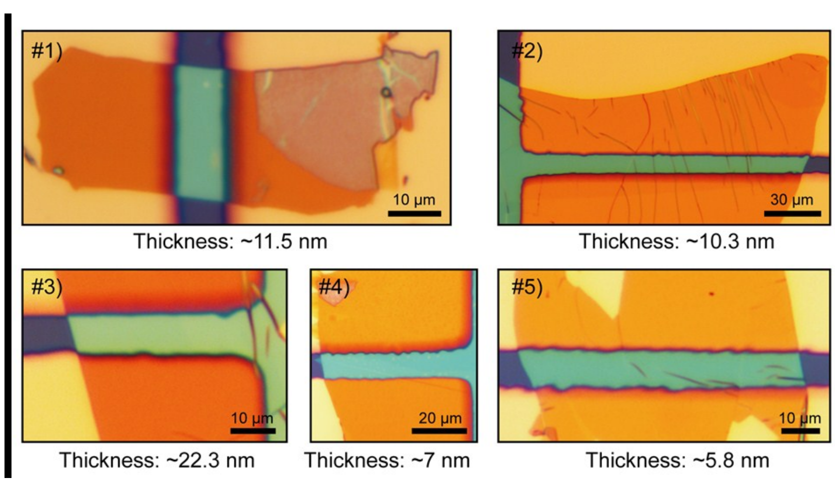

Figure S4: Optical pictures of five thin InSe photodetectors with various thicknesses and labeled #1 to #5 investigated in this work.

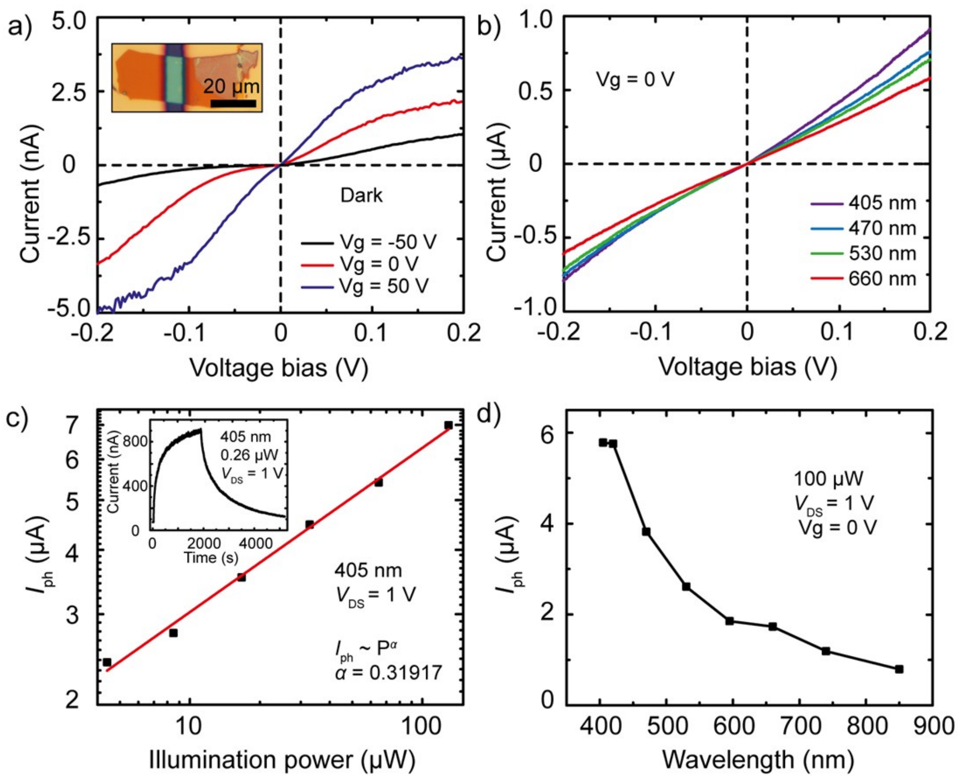

Figure S5: The optoelectronic characterization in vacuum ($0.5\text{-}\times10^{-6}$ mbar - $1\text{-}\times10^{-6}$ mbar) of the InSe photodetector (#1). (a) The *I*-*V* curves of the InSe photodetector in dark condition with the gate voltage V_g = -50 V, 0 V, and 50 V, respectively. (b) The *I*-*V* curves of the InSe photodetector under various illumination wavelength with the same power density of 354 W m^{-2}. (c) The photocurrent versus illumination intensity (~ 4 – 128 μW) plotted in log-log scale with the 405 nm illumination. The inset figure is an *I*-t curve for the InSe photodetector. (d) The photocurrent evolution with different wavelength under the illumination density of 354 W m^{-2} at V_{DS} = 1 V.

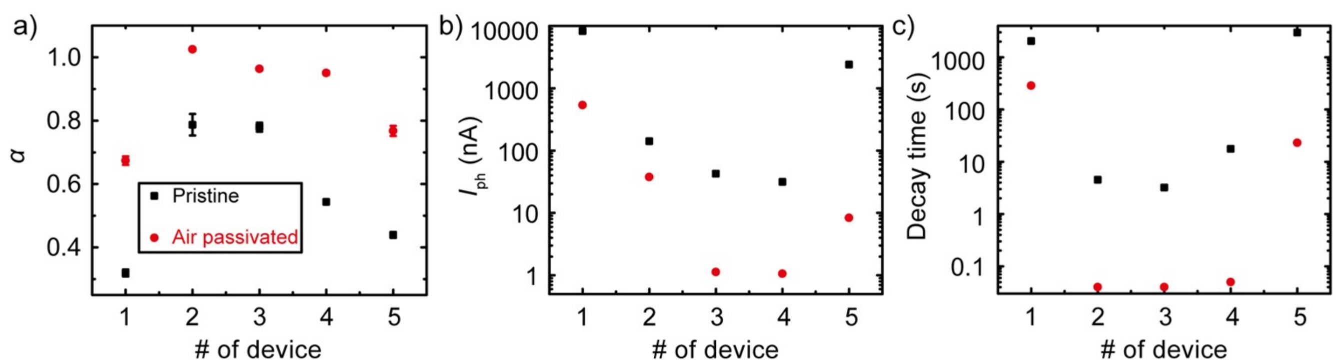

Figure S6: Statistic results of five InSe photodetectors (in Figure S4) before and after air passivation. α (a), photocurrent (b), and decay time (c) of five InSe photodetectors with pristine state and after air passivation under the same measurement conditions. All the tested InSe photodetectors share the same manner when exposed to air.

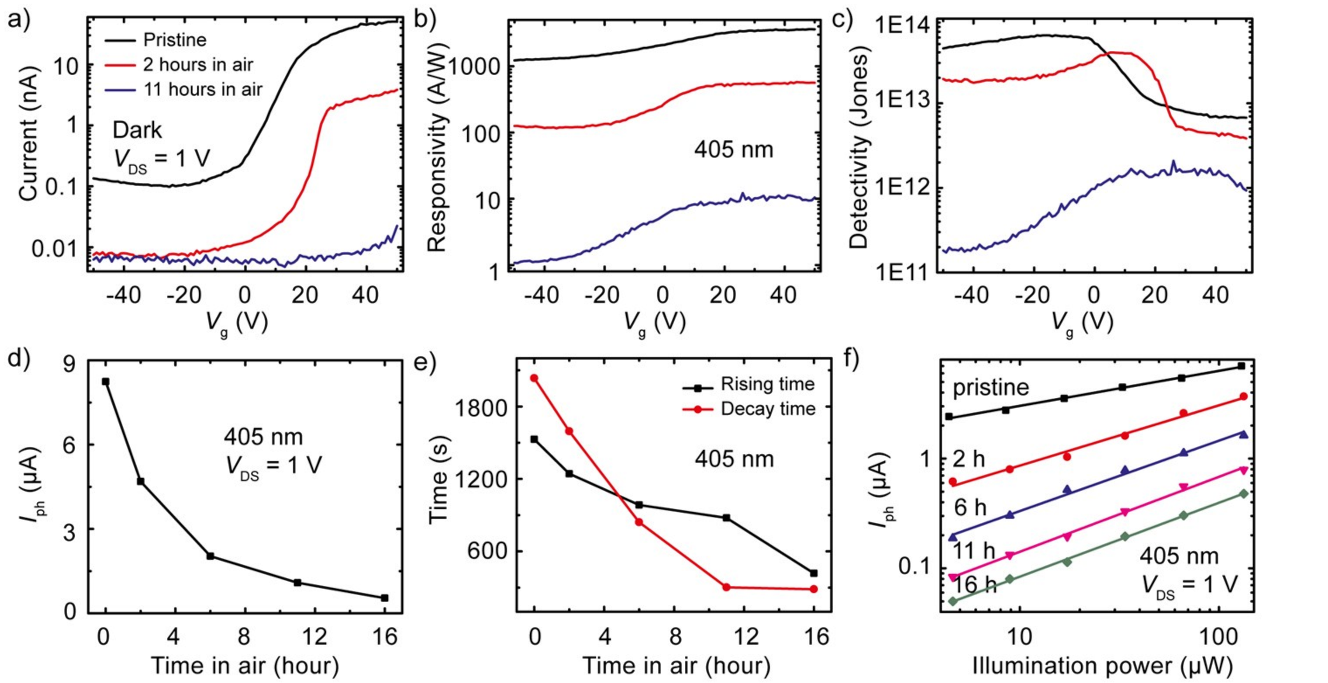

Figure S7: Time-dependent performance of the InSe photodetector (#1) when exposed to air. The gate-dependence of the InSe photodetector in dark (a), photoresponsivity (b) and detectivity (c) of 405 nm at 0.92 W m^{-2} illumination after exposed to air 0 h, 2 h, 11 h. The evolution of photocurrent (at 906 W m^{-2}), rising and decay time (at 906 W m^{-2}), and photocurrent – illumination intensity dependence of 405 nm light as a function of exposure time in air.

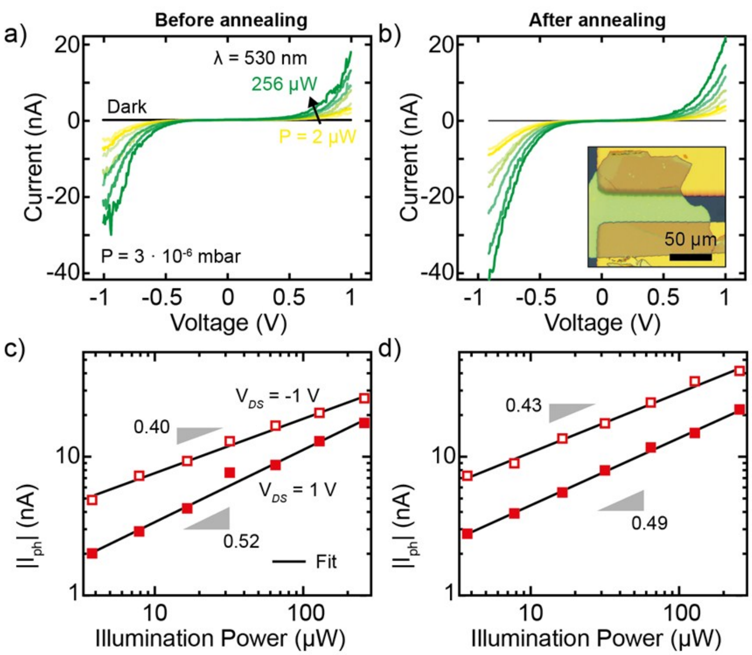

Figure S8: (a-b) The *I-V* curves of a InSe photodetector in dark condition and under illumination at 530 nm and at different powers recorded in vacuum (~10^{-6} mbar) before and after annealing at 100 ℃ for 2 hours keeping the same vacuum level. c-d) Absolute value of the photocurrent extracted from the *I-V*s of panels (a) and (b) as a function of the illumination power. The photocurrent extracted at a voltage of 1 V and -1 V is fitted to a power law (black line).

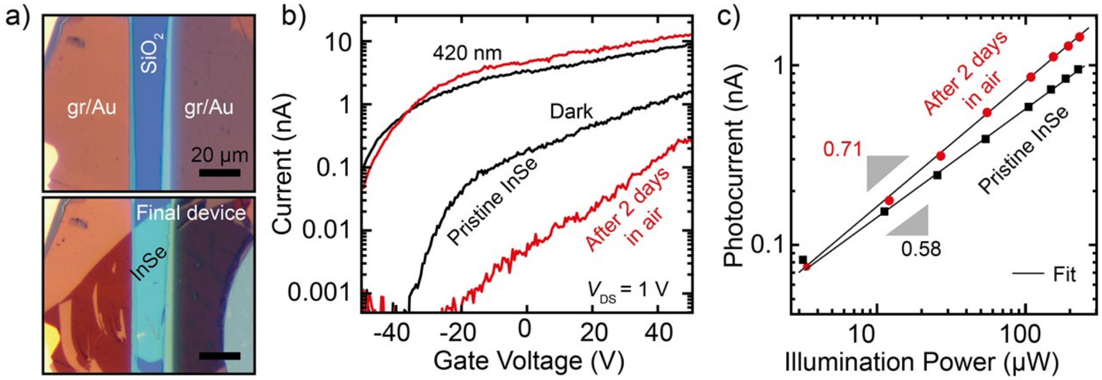

Figure S9: Time-dependent performance of a graphite-InSe-graphite photodetector when exposed to air.

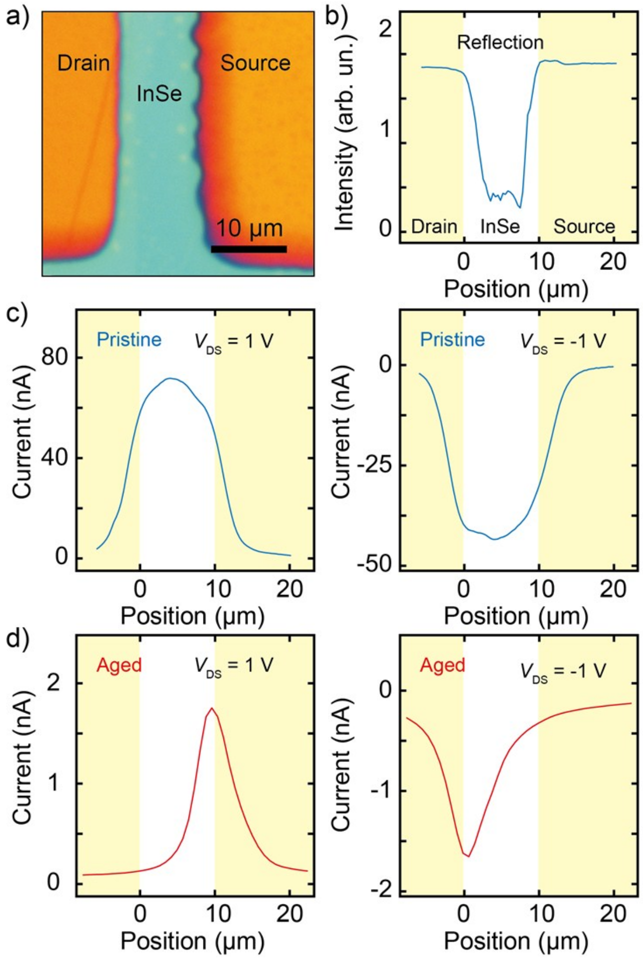

Figure S10: a) Optical image of device #4. b) Intensity of the laser reflection from the sample recorded during the scanning photocurrent measurements of panels c and d. c-d) Spatially resolved photocurrent at $V_{ds} = \pm 1$ V of device #4 recorded just after fabrication (blue) and after 10 days in air (red).

Section S4 – Kinetics processes in the InSe photocurrent generation model

The schematic band diagram proposed for InSe photodetectors in presence of traps is shown in Fig. S11a. The photogating mechanism that dominates the photocurrent generation in pristine InSe devices as we discussed in the main text, is based on the trapping of the minority charge carriers (in the case of InSe are holes). Figure S11b shows a diagram that includes only a set of traps, with density N_t and located at an energy E_t. To model the rising and decay of the photocurrent when respectively switching on and off the external illumination, we focus on two kinetic processes: the capture of holes by a trapping level and the emission of holes from the trap (schematically represented by the dashed arrows in the figure). The first process gives an increase of the photocurrent through photogain and is related to the rising time τ_{on}, while the second process leads to a decrease of the photocurrent and determines the decay time τ_{off}.

When illuminating an InSe photodetector previously kept in dark the process that leads to the equilibrium state is the trapping of holes by the previously empty traps (*i.e.* filled with electrons). The trapping rate, $r_t = 1/\tau_t$, is described by the equation:

$$r_t = v \cdot \sigma_p \cdot p \cdot N_t \cdot f, \qquad \text{(S1)}$$

where v is the thermal velocity of holes, σ_p is the cross section for holes, p is the free holes density under illumination and $N_t \cdot f$ gives the number of empty (*i.e.* filled with electrons) traps.

Contrarily, when the illumination is removed the favored process is the detrapping of holes and the detrapping rate, $r_d = 1/\tau_d$, can be described by equation:

$$r_d = v \cdot \sigma_p \cdot N_t \cdot (1\text{-}f) \exp[(E_{VB} - E_t)/kT], \qquad \text{(S2)}$$

where $N_t \cdot (1\text{-}f)$ gives the number of filled traps and E_{VB} is the energy of the valence band maximum.

From the data shown in Fig. 3a of the main text we estimate a rising time τ_{on} = 77 s and a decay time τ_{off} = 3.2 s. This corresponds to the situation in which the detrapping process is faster than the trapping $r_d > r_t$ that can be rewritten as $r_d / r_t > 1$. Using this condition and substituting equations S1 and S2, we can write the relation:

$$\frac{exp[(E_{VB} - E_t)/kT]}{p} \cdot \frac{1-f}{f} > 1. \qquad \text{(S3)}$$

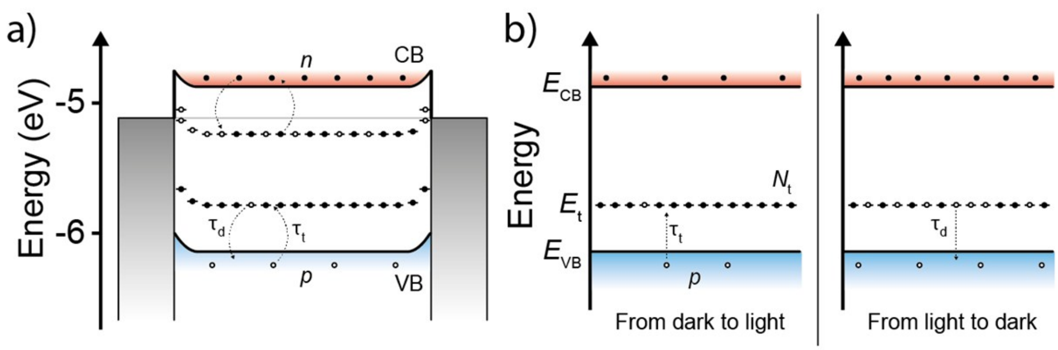

Figure S11: (a) Schematic band diagram of a InSe photodetector with traps. Depicted there are the valence (VB) and conduction band (CB) of InSe, the gold elecrodes and the Fermi energy and a set of hole trapping levels (whose density is P_t) and electron trapping levels (density N_t). The density of free electrons and free holes are respectively n, p. (b) Schematic band diagram of a InSe with only one set of traps with density P_t. The left schematic depicts the trapping of holes when exposing the InSe to external illumination and the right scheme shows the detrapping of holes when the external illumination is removed.